

# Investigation of Boost Converter to Track Maximum Power Point for the Doubly Fed Induction Generators in the Wind Farm

Tabib Yousefi<sup>1\*</sup>, Abdolreza Tavakoli<sup>2</sup>, Farzad Arasteh<sup>3</sup> and Abdollah Aghazadeh<sup>3</sup>

<sup>1</sup>Technical and Vocational University, Rasht Branch, Rasht, Iran; tabibyosefi@gmail.com

<sup>2</sup>Department of Electrical Engineering, Lahijan Branch, Islamic Azad University, Lahijan, Iran; tavakoli@liau.ac.ir

<sup>3</sup>Electronic Branch, Islamic Azad University, Tehran, Iran; farasteh149@yahoo.com, abdollaaghazade@yahoo.com

## Abstract

**Background/Objectives:** In this paper, tracking the Maximum Power Point for the Doubly Fed Induction Generators in the Wind Farm through a boost converter is analyzed. **Methods/Statistical Analysis:** Achieving maximum power at wind farm and subsequently improving power quality disturbances in power systems is very important. Methods used to track the maximum power point are: 1-TSR control 2-P&O control 3-ORB control This paper, presents a combination of P&O and ORB control method to extract maximum power at Doubly Fed Induction Generators (DFIG). **Findings:** In this method, there is no need to anemometer and the recent information of wind speed. In addition, the little Fluctuations near the maximum power point, is an improved factor in this technique. Simulation results using Matlab software, proves the truth of this claim.

**Keywords:** Boost Converter, Doubly Fed Induction Generators, Track Maximum Power Point, Wind Farm

## 1. Introduction

Due to the limited resources of fossil fuels, the problem of pollution from these sources and also increasing rate of energy prices, using renewable energy, especially wind energy, has become a very important matter. So, the main goal of this article is tracking the maximum power point of a wind turbine in order to increase efficiency and Economic benefits from the exploitation of these resources. In recent decades, many researches to use renewable sources have been done and also it is expected to extract more energy from wind power in the future.

In Wind farms due to variable speed of wind, the output power is variable. TSR method measures the ratio of turbine speed to wind speed, so, the rotor speed can be adjusted according to the changes in the actual speed of the wind and in this way the output power of the turbine is at the optimal level. In other words, in order to achieve MPP<sup>4</sup>, the rotor speed is adjusted through wind speed changes<sup>1</sup>.

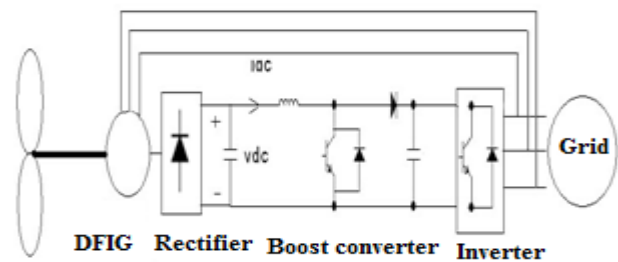


Figure 1. Wind conversion system.

Mechanical power of the turbine with different wind speeds is shown in Figure 2. The disadvantages of this method are requirement to anemometer and the prior information of wind speed<sup>2-7</sup>. The P&O method without anemometer, adjusts turbine speed by comparing successive output power. This method is used in small-scale wind farms that will increase reliability and reduce costs. But disadvantage of this method is slow response to wind speed changes especially for the turbines with high inertia which causes fluctuations to achieve maximum

\* Author for correspondence

power at wind farm and reduce productivity<sup>8-14</sup>.

The ORB method ensures the Maximum Power Point through Optimal Relationship Between the system parameters. It's not needed to measure wind speed in this method and also the maximum amplitude of the oscillations near MPP is reduced. So, this is a qualified manner to reach MPP<sup>15</sup>. But, this method needs a lot of space to process data and the primary data is also essential.

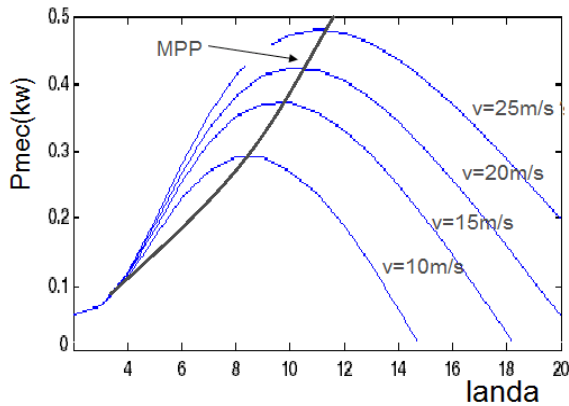


**Figure 2.** Mechanical power of the turbine with different wind speed.

In this paper, the combination of P&O and the ORB methods has been used to track maximum power point of the double fed induction generator in the wind farm. In this regard, through advanced P&O controlling Method, the optimum relationship between dc voltage and current in different wind speed is calculated and then ORB method optimizes the parameters to achieve MPP. The mentioned method does not need to anemometer and the previous conditions of wind and also can be applied to small and large scales of wind farms. Overall process of the simulation is conducted According to Figure 1. Output power of the Double-fed induction generator in the wind farm is delivered to grid through a diode bridge rectifier, a boost converter and an inverter. In addition, boost converter controls dc voltage and current and applies dc current to inverter. The second section of this article is about wind farm Information and the third part discusses about the ways to achieve maximum power point and the proposed methods. Section (4) includes the simulation results with MATLAB software and section (5) concludes this study and suggests new subjects.

## 2. The Characteristics of Wind Farms

### 2.1 Mechanical Properties

Wind turbine mechanical power is obtained from the following equation<sup>16-17</sup>.

$$P = \frac{1}{2} \rho A C_p V_w^3 \quad (1)$$

In the above equation, “ $\rho$ ” the air density, “ $C_p$ ” the power coefficient and “ $A$ ” is the cross section of the turbine blade. Pitch angle (ratio of the turbine speed to the wind speed “ $\lambda$ ”) is as below.

$$\lambda = \frac{r\Omega}{V_w} \quad (2)$$

In this regard, “ $r$ ” the radius of the rotor blades, “ $\Omega$ ” the turbine rotor speed and “ $v_w$ ” is the wind speed. The above Equations show that the maximum power is proportional to the cube of wind speed.

$$P_{\max} \propto V_w^3 \propto \Omega_{opt}^3 \quad (3)$$

### 2.2 Electrical Characteristics

In a double-fed induction generator with constant flux, induced motive force has linear relation with speed.

$$E = K_e \Phi \omega \quad (4)$$

In this regard, “ $\Phi$ ” and “ $K_e$ ” are constant and the terminal voltage of the generator is obtained from the following equation.

$$V_{ac} = E - I_{ac}(R_s) + j\rho\Omega L_s \quad (5)$$

In Equation (5), “ $V_{ac}$ ” the terminal phase voltage, “ $I_{ac}$ ” phase current, “ $R_s$ ” stator resistance, and “ $L_s$ ” is the rotor inductance<sup>18</sup>.

$$V_{dc} = \frac{3\sqrt{3}}{\pi} V_{ac} \quad (6)$$

$$V_{dc} \propto \Omega \quad (7)$$

And finally, the following Equations are concluded from the mentioned Equations.

$$I_{dc} \propto V_{dc}^2 \quad (8)$$

$$P \propto V_{cd} \quad (9)$$

In Figure 3,  $I_{dc}$  versus  $V_{dc}^2$  curve based on the simulation results for different wind speeds is shown. According to the Equation (10), “a” is constant but  $I_{dc}$  is dependent to  $V_{dc}^2$  and  $\theta$ .

$$I_{dc} = (atg\theta)V_{dc}^2 \tag{10}$$

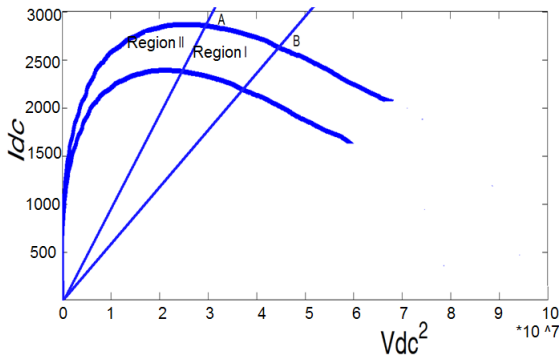


Figure 3.  $I_{dc}$  versus  $V_{dc}^2$  curve in different wind speed.

### 3. The Method used To Achieve Maximum Power

In this paper, the combination of P&O and the ORB methods in order to extract maximum power has been studied. So, According to Equation (10), the optimum dc voltage and current is calculated using P&O algorithm and then, these values are controlled with ORB method. The Flowchart of the process is shown in Figure 4, Figure 5 and 6 describes about the Control block diagram of P&O and ORB method. In addition, in optimal condition, Equation (10) changes as below.

$$I_{dc-opt} = (atg\theta)V_{dc-opt}^2 \tag{11}$$

$I_{dc-opt}$  is the Optimized current,  $V_{dc-opt}$  is the optimum voltage, “a” can be considered constant and  $\theta$  is calculated

based on the comparative analysis of output power. According to the flowchart in Figure 4, the process of tracking maximum power point can be divided into two parts.

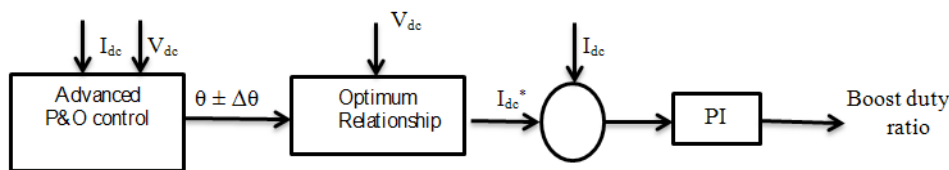


Figure 5. P&O control block diagram.

### 3.1 Training Mode (P&O)

Assume the area above line “A” in Figure 3 as region (II), and under the line is region (I). If  $\theta$  reaches to  $\theta_{opt}$ , the maximum power is extracted. So, in stable wind speed,  $\theta$  should be decreased in region (II) and increased in region (I) in order to get  $\theta_{opt}$ . This process is outlined in the flowchart of the P&O method. Figure 5 and 6 shows the block diagram of the P&O and ORB control method.

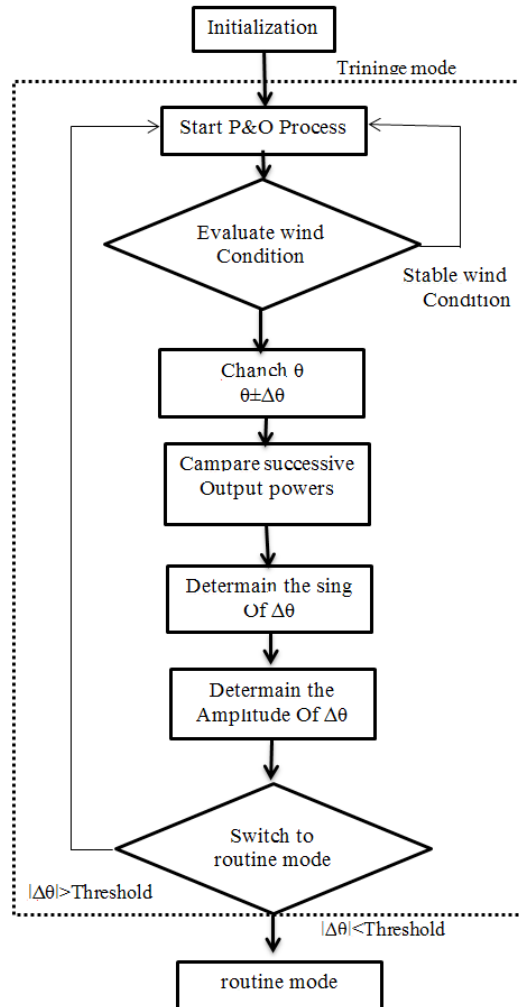


Figure 4. Flow control process.

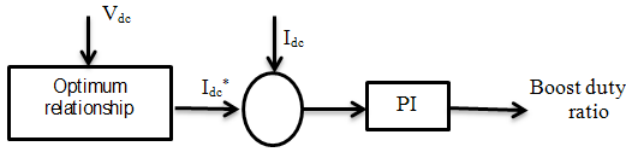


Figure 6. ORB control block diagram.

### 3.1.1 Determining the Sign of $\Delta\theta$

At First, assume a reference angle ( $\theta_{ref}$ ) and calculate the power and then by applying successive changes ( $\theta_{ref} \pm \Delta\theta$ ), related powers should be calculated. At each step,  $\Delta P$  should also be calculated. So, two different states will happen.

If the sign of  $\Delta P$  is positive, it means that the changes are in region (I), and  $\theta$  should be increased to arrive at  $\theta_{opt}$  ( $sign = +1$ ). Unlike, if  $\Delta P$  is negative, it means that the changes are in region (II), and  $\theta$  should be decreased to arrive at  $\theta_{opt}$  ( $sign = -1$ ).

$$sign[n] = \begin{cases} +1 \rightarrow area(I) \\ -1 \rightarrow area(II) \end{cases} \quad n > 0 \quad (12)$$

However, if  $sign[n] = sign[n-1]$ ,  $\theta$  is close to  $\theta_{opt}$ .

### 3.1.2 Determining the Amplitude of $\Delta\theta$

The Process of changes in the amplitude of  $\Delta\theta$  is Similar to the changes in its sign.

$$Amplitude[m] = \begin{cases} +1 \rightarrow area(I) \\ -1 \rightarrow area(II) \end{cases} \quad m > 0 \quad (13)$$

In Equation (12), n is for the changes with larger steps and m Represent smaller steps for  $\Delta\theta$  in Equation (13).

$$Amplitude[m] = Amplitude[m-1] \quad (14)$$

If Equation (14) is satisfied, it means that  $\theta$  has converged to  $\theta_{opt}$  and

$$0 \leq \frac{\sum_1^m Amplitude[K]}{m!} \leq 1 \quad (15)$$

m is the number of iterations.

## 3.2 Routine Mode (ORB)

If Equation (15) is satisfied, ORB control approach replace with P&O process. The Values of  $a, n, m, \theta_{ref}$  is represented in Table 1. In short, the process starts with determining  $V_{dc-opt}$  and  $\theta_{opt}$  with P&O control method and then according to Equation (11),  $I_{dc-opt}$  is calculated. This current is compared with the circuit current and eventually  $I_{dc-opt}$  and  $V_{dc-opt}$  is applied to the boost converter.

## 4. Simulation results in MATLAB software

Control parameters data in the simulation process is presented in table (1) and double fed induction generator parameters and wind turbine data is offered in Table (2). The output Waveforms are analyzed in the steady state condition. Figure 7 shows wind speed Variations versus time and Figure 8 is the maximum output power considering wind speed changes. As can be seen, the output power follows wind speed changes. So, increasing in wind speed, cause an increment in the output power. Unlike, decreasing in wind speed, cause a decrement in the output power. Figure 9 presents the gradual changes for  $\theta$  in a specific wind speed. At the beginning,  $\theta$  starts with a small angel and gradually get close to  $\theta_{opt}$ . It's visible that, hiring P&O method reduces the amplitude of fluctuations around  $\theta_{opt}$ . Ultimately by finishing P&O process,  $\theta$  arrives at  $\theta_{opt}$ .

Table 1. Control parameters of the simulation

$4 \times 10^{-5}$	a
4	n
50	m
$10^0$	$\theta_{ref}$
0.4	$\Delta\theta_{TH}$

Table 2. Wind turbine parameters of the double fed induction generator

9MW	Nominal Power
575 v	Nominal Voltage
0.023pU, 0.18pU	Resistance and the Inductance of the Stator
$4 \frac{m}{s}$	Minimum Wind Speed
$11 \frac{m}{s}$	Maximum Wind Speed
60 HZ	Frequency

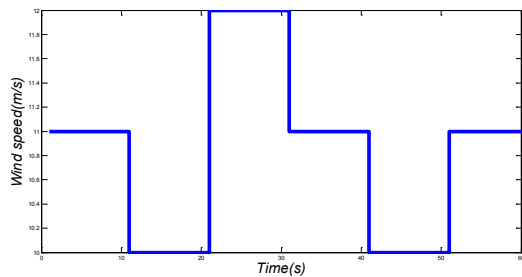


Figure 7. Variation of wind speed versus time.

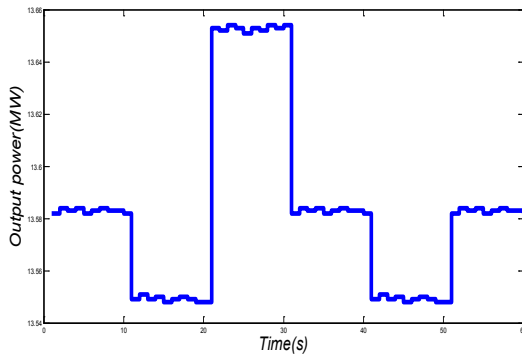


Figure 8. Output power changes according to wind speed conditions.

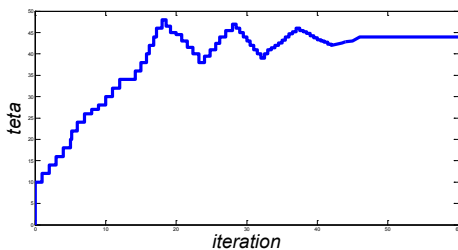


Figure 9. Gradual changes of  $\theta$  to achieve  $\theta_{opt}$  in a certain wind speed.

## 5. Conclusion

In this paper, the combination of P&O and the ORB control methods to Track maximum power point of a wind farm with Double-fed induction generator has been analyzed. Therefore, Advanced P&O Method calculates the optimum dc voltage and current and then the process of controlling optimum voltage and current is managed through ORB method. With the Mentioned Approach, Achieving maximum power even under unsteady wind

speed is ensured. Online updating, No need to prior information of Wind and no anemometer are the other benefits of this approach. Result of the simulation through MATLAB software demonstrates the acceptable performance of the approach.

## 6. References

1. Mirecki A, Roboam X, Richardeau F. Architecture complexity and energy efficiency of small wind turbines. *IEEE Transactions on Industrial Electronics*. 2007; 54(1):660-70.
2. Manwell JF, McGowan JG, Rogers AL. *Wind energy explained: Theory, design and application*. John Wiley & Sons; 2010.
3. Thiringer T, Linders J. Control by variable rotor speed of a fixed-pitch wind turbine operating in a wide speed range. *IEEE Transactions on Energy Conversion*. 1993; 8(3): 520-6.
4. Hilloowala RM, Sharaf AM. A rule-based fuzzy logic controller for a PWM inverter in a standalone wind energy conversion scheme. *IEEE Transactions on Industry Applications*. 1996; 32(1):57-65.
5. Chedid R, Mrad F, Basma M. Intelligent control of a class of wind energy conversion systems. *IEEE Transactions on Energy Conversion*. 1999; 14(4):1597-604.
6. Johnson KE, et al. Methods for increasing region 2 power capture on a variable-speed wind turbine. *Journal of Solar Energy Engineering*. 2004; 126(4):1092-100.
7. Johnson KE, et al. Control of variable-speed wind turbines: Standard and adaptive techniques for maximizing energy capture. *IEEE Control Systems*. 2006; 26(3):70-81.
8. Wang Q, Chang L. An intelligent maximum power extraction algorithm for inverter-based variable speed wind turbine systems. *IEEE Transactions on Power Electronics*. 2004; 19(5):1242-9.
9. Buehring IK, Freris LL. Control policies for wind-energy conversion systems. *IEE Proceedings C (Generation, Transmission and Distribution)*; 1981.
10. Datta R, Ranganathan VT. A method of tracking the peak power points for a variable speed wind energy conversion system. *IEEE Transactions on Energy Conversion*. 2003; 18(1):163-8.
11. Simoes MG, Bose BK, Spiegel RJ. Fuzzy logic based intelligent control of a variable speed cage machine wind generation system. *IEEE Transactions on Power Electronics*. 1997; 12(1):87-95.
12. Simoes MG, Bose BK, Spiegel RJ. Design and performance evaluation of a fuzzy-logic-based variable-speed wind generation system. *IEEE Transactions on Industry Applications*. 1997; 33(4):956-65.
13. Koutroulis E, Kalaitzakis K. Design of a maximum power tracking system for wind-energy-conversion applications. *IEEE Transactions on Industrial Electronics*. 2006; 53(2):486-94.

14. Kazmi SMR, et al. A novel algorithm for fast and efficient speed sensor less maximum power point tracking in wind energy conversion systems. *IEEE Transactions on Industrial Electronics*. 2011; 58(1):29-36.
15. Bhowmik S, Spee R, Enslin JHR. Performance optimization for doubly fed wind power generation systems. *IEEE Transactions on Industry Applications*. 1999; 35(4):949-58.
16. Kundur P. Power system stability and control. In: Balu NJ, Lauby MG. Editors. Vol. 1. New York: McGraw-hill; 1994.
17. Izadbakhsh M, et al. Dynamic analysis of PMSG wind turbine under variable wind speeds and load conditions in the grid connected mode. *Indian Journal of Science and Technology*. 2015; 8(14).